Materials Science and Engineering C 57 (2015) 31–37

Contents lists available at ScienceDirect

Materials Science and Engineering C

journal homepage: www.elsevier.com/locate/msec

Immobilization of cholesterol oxidase on magnetic fluorescent core-shell-structured nanoparticles

Jun Huang *, Huichao Liu, Peipei Zhang, Pengfei Zhang, Mengshi Li, Liyun Ding

National Engineering Laboratory for Fiber Optic Sensing Technology, Wuhan University of Technology, Wuhan 430070, China
Key Laboratory of Fiber Optic Sensing Technology and Information Processing (Wuhan University of Technology), Ministry of Education, Wuhan 430070, China

ARTICLE INFO

Article history:
Received 3 February 2015
Received in revised form 24 June 2015
Accepted 22 July 2015
Available online 26 July 2015

Keywords:
Magnetic fluorescent SiO_2 nanoparticles
COD immobilization
Stability
Fiber optic biosensor

ABSTRACT

The magnetic fluorescent core-shell structured nanoparticles, Fe_3O_4@SiO_2(F)@meso–SiO_2 nanoparticles, were prepared. Cholesterol oxidase (COD) was immobilized on their surface to form Fe_3O_4@SiO_2(F)@meso–SiO_2@COD nanoparticles. Optimal immobilization was achieved with 2.5% (v/v) APTES, 2.0% (v/v) GA, 10 mg COD (in 15 mg carrier) and solution pH of 7.0. Fe_3O_4@SiO_2(F)@meso–SiO_2@COD nanoparticles showed maximal catalytic activity at pH 7.0 and 50 °C. The thermal, storage and operational stabilities of COD were improved greatly after its immobilization. After the incubation at 50 °C for 5 h, the nanoparticles and free COD retained 80% and 46% of its initial activity, respectively. After kept at 4 °C for 30 days, the nanoparticles and free COD maintained 86% and 65% of initial activity, respectively. The nanoparticles retained 71% of its initial activity after 7 consecutive operations. Since Fe_3O_4@SiO_2(F)@meso–SiO_2@COD nanoparticles contained tris(2,2-bipyridyl)dichloro-ruthenium(II) hexahydrate ($Ru(bpy)_3Cl_2$) and were optical sensitive to oxygen in solution, it might be used as the sensing material and has the application potential in multi parameter fiber optic biosensor based on enzyme catalysis and oxygen consumption.

1. Introduction

It is well known that high cholesterol level in blood is associated with the clinical disorders such as hypertension, arteriosclerosis, myocardial infarction, nephrosis and diabetes mellitus. Therefore the determination of cholesterol using rapid, cheap and reliable methods is of great importance in clinical diagnosis. Fiber optic biosensors have many advantages including high sensitivity, fast response, immunity from electrical interference and low cost, and could be the effective way to determine cholesterol concentration. Cholesterol oxidase (COD) catalyzes the oxidation of cholest-5-en-3-one and then the isomerization to cholest-4-en-3-one [1]. For the fiber optic biosensor based on cholesterol oxidase catalysis, the sensing performance depends mainly on the enzyme properties. As a native enzyme, COD has the drawbacks of high cost, poor stability and resource shortage. However, the properties of COD can be greatly improved after its immobilization on suitable carriers due to the fact that the immobilized enzyme offers several advantages such as its reuse, improved stability and ease removal from the reaction medium.

A certain amount of work has been done on COD immobilization. Chen et al. used functionalized sepharose particles as the carrier to immobilize COD [2]. The thermal, pH and storage stabilities of COD were increased by immobilization. Yapar et al. immobilized COD in conducting network via complexation of chitosan with alginic acid [3]. The immobilized COD still maintained 63% of its initial activity after 44 measurements, showing an excellent operational stability. Gilles et al. immobilized COD on to Fe_3O_4 magnetic nanoparticles [4]. The immobilized enzyme exhibited a better tolerance to pH and temperature, and it also had an improved stability. In addition, COD has been immobilized on perlite [5], polyaniline films [6], hollow fiber [7], silk mat [8], functional polymetric supports [9], hydrogel [10], Alkylamine glass beads [11], mesoporous silica materials [12] and sol-gel film [13]

SiO_2 nanoparticles have the advantages of ease to prepare, good biocompatibility and large specific surface area [14,15]. Fluorescent silica nanoparticles offer significant advantages compared to free dyes due to the fact that the encapsulation of luminescent molecules in silica nanoparticles often increases their photostability and emission quantum yield [16–19]. The reported sensing materials for fiber optic biosensor based on enzyme catalysis usually consist of two parts [20–22], the optical sensing part and catalytic enzyme part. If the enzyme is immobilized on the fluorescent SiO_2 nanoparticles containing oxygen sensing photosensitizer and these complex nanoparticles are used as the sensing materials for fiber optic biosensor, the catalysis effect of enzyme can arrive at the photosensitizer directly and the performance of fiber optic biosensor will be improved. The complex nanoparticles with the magnetic core will be beneficial to the isolation of the immobilized enzyme from the reaction mixture. If different enzymes were immobilized on magnetic luminescent silica nanoparticles and

* Corresponding author at: National Engineering Laboratory for Fiber Optic Sensing Technology, Wuhan University of Technology, Wuhan 430070, China.
E-mail address: hjun@whut.edu.cn (J. Huang).

http://dx.doi.org/10.1016/j.msec.2015.07.038
0928-4931/

the enzyme performance was controlled, it will be possible to develop the multi parameter fiber optic biosensor based on enzyme catalysis and oxygen consumption.

In this work, the magnetic fluorescent core-shell structured nanoparticles, Fe_3O_4@SiO_2(F)@meso–SiO_2 nanoparticles, were prepared. The core of nanoparticles consisted of a single Fe_3O_4 nanoparticle encapsulated in fluorescent dye $Ru(bpy)_3Cl_2$ co-doped nonporous silica, their shell was made from ordered mesoporous silica. COD was immobilized on their surface to form Fe_3O_4@SiO_2(F)@meso–SiO_2@COD nanoparticles. Immobilization conditions were investigated and optimized. The properties of Fe_3O_4@SiO_2(F)@meso–SiO_2@COD nanoparticles such as catalytic activity as a function of pH and temperature, thermal, storage and operational stabilities were studied. Since Fe_3O_4@SiO_2(F)@meso–SiO_2@COD nanoparticles have improved catalytic performance and oxygen sensing property, they will have the application potential in multi parameter fiber optic biosensor based on enzyme catalysis and oxygen consumption. To the best of our knowledge, there has been no report on this kind of magnetic materials with the properties of enzymatic catalysis and optical oxygen sensing.

2. Experimental

2.1. Chemicals

COD (E.C. 1.1.3.6, 20 U/mg), Cholesterol, $Ru(bpy)_3Cl_2$ (99.0%), hexadecyltrimethyl ammonium bromide (CTAB) were purchased from Aldrich-Sigma. 3-aminopropiltrietoxysilane (APTES) was purchased from Alfa Aesar. Tetraethoxysilane (TEOS) and glutaraldehyde (GA) (25% aqueous solution) were purchased from Sinopharm Chemical Reagent Co.. All reagents were with analytical grade and used without further purification. Double-distilled water was used throughout the experiments.

2.2. Preparation of Fe_3O_4@SiO_2(F) nanoparticles

The magnetic Fe_3O_4 nanoparticles were prepared using the method of Massart [23]. 4 mg of $Ru(bpy)_3Cl_2.6H_2O$ was reacted with 30 μL of APTES in 5 mL of ethanol under dark condition for 24 h. The prepared fluorescent agent precursor solution was kept at 4 °C. 155 mL of ethanol, 27 mL of H_2O, 8 mL of ammonia, 5 mL of fluorescent agent precursor solution, and 4 mL of Fe_3O_4 nanoparticles solution were added in a 250 mL conical flask consecutively. Finally, 0.44 mL of TEOS was added slowly. After ultrasonic treatment for 10 min, the mixture was stirred at 25°C for 6 h. The product was washed with H_2O to neutral and dry in vacuum at 60°C

2.3. Preparation of Fe_3O_4@SiO_2(F)@meso–SiO_2 nanoparticles

The Fe_3O_4@SiO_2(F)@meso–SiO_2 nanoparticles were prepared by a modified stöber sol-gel method [24]. 0.20 g of Fe_3O_4@SiO_2(F) nanoparticles, 0.17 g of CTAB, 0.5 mL of ammonia, 25 mL of ethanol were added in 54 mL of H_2O consecutively. 0.3 mL of TEOS was added slowly. After ultrasonic treatment for 10 min, the mixture was stirred at 25°C for 8 h. After the particles were magnetically separated and washed with ethanol twice, they were refluxed in acidic ethanol at 100°C under N_2 for 24 h to remove CTAB. The product was washed with ethanol to neutral and dry in vacuum at 60°C.

2.4. Preparation of Fe_3O_4@SiO_2(F)@meso–SiO_2@COD nanoparticles

15 mg Fe_3O_4@SiO_2(F)@meso–SiO_2 nanoparticles was added into 4 mL 2.5% (v/v) APTES solution and stirred at 25°C for 24 h. The modified nanoparticles were washed with H_2O and redispersed in 3.68 mL phosphate buffer solution (PBS, 0.01 mol/L, pH = 7.3). 0.32 mL of 25% (v/v) GA was added in the mixture and stirred for 1.5 h. The mixture was washed with neutral PBS for several times. The activated Fe_3O_4@SiO_2(F)@meso–SiO_2 nanoparticles were obtained after centrifugation. For the immobilization of COD, 2 mL of COD (5 mg/mL) was allowed to contact with the activated Fe_3O_4@SiO_2(F)@meso–SiO_2 nanoparticles in a tube at 4°C for 12 h with occasional shaking. Then the Fe_3O_4@SiO_2(F)@meso–SiO_2 nanoparticles were washed with PBS buffer (0.05 M, pH = 7.0) thoroughly to remove free COD and Fe_3O_4@SiO_2(F)@meso–SiO_2@COD nanoparticles were obtained and stored in PBS buffer (0.05 M, pH = 7.0).

Followed Bradford method [25], by subtracting the residual free GOD content in the solution from the initial free GOD content the amount of GOD protein loaded onto the porous fluorescent SiO_2 nanoparticles was measured.

2.5. Assay of COD activity

The activity of free COD and Fe_3O_4@SiO_2(F)@meso–SiO_2@COD nanoparticles were determined spectrophotometrically [9] 2.5 mL of cholesterol solution was contacted with free COD or Fe_3O_4@SiO_2(F)@COD nanoparticles. After incubation of 2 min, 2.5 mL of solution containing 4-aminoantipyrine, phenol, peroxidase were added and waited for 10 min to complete quinoneimine dye formation. The COD activity was measured, in triplicate, by recording the absorbance of the red dye at 500 nm at which the dye complex exhibited its maximal adsorption. One unit of COD activity converts 1.0 μmol of cholesterol to 4-cholesten-3-one per min at pH 7.0 and 25 °C.

2.6. Stability of COD

To study the thermal stability of free COD and Fe_3O_4@SiO_2(F)@meso–SiO_2@COD nanoparticles, enzyme activity was determined in different time of incubation at 60 °C. The storage stability of free COD and Fe_3O_4@SiO_2(F)@meso–SiO_2@COD nanoparticles was investigated by storing them at 4 °C for 30 days and determining their residual activity every five days.

To investigate the operation stability of Fe_3O_4@SiO_2(F)@meso–SiO_2@COD nanoparticles, several consecutive operation cycles were performed by oxidizing cholesterol. At the end of each oxidation cycle, PBS buffer (0.1 M, pH 7.0) was used to wash the nanoparticles for several times and the procedure was carried out repeatedly with a fresh aliquot of substrate.

2.7. Characterizations

The morphologies of Fe_3O_4@SiO_2(F)@meso–SiO_2 nanoparticles and Fe_3O_4@SiO_2(F)@meso–SiO_2@COD nanoparticles were observed using a transmission electron microscopy (JEM-100 CXII, JEOL, Japan). Pore size and porosity measurements were performed by the Brunauer–Emmett–Teller (BET) method on an ASAP 2020 instrument. The magnetic properties of nanoparticles were characterized using 4HF vibrating sample magnetometer (VSM). The fluorescence spectra were recorded using a fluorescence spectrophotometer (F-4500, HITACHI, Japan). FT–IR spectrum was recorded on a Thermo Nicolet Nexus FT–IR spectrometer with the standard KBr pellet method. The activities of Fe_3O_4@SiO_2(F)@meso–SiO_2@COD nanoparticles were measured by spectrophotometer (UV-2450, Shimadzu, Japan).

3. Results and discussion

3.1. Preparation and characterization of Fe_3O_4@SiO_2(F)@meso–SiO_2 nanoparticles and Fe_3O_4@SiO_2(F)@meso–SiO_2 @COD nanoparticles

Fe_3O_4@SiO_2(F)@meso–SiO_2 nanoparticles were prepared by a multistep process. Monodisperperse superparamagnetic Fe_3O_4 nanoparticles were first prepared using the method of Massart [23]. Then the prepared Fe_3O_4 nanoparticles were coated with a layer of silica. The formation of SiO_2 nanoparticles consisted of hydrolysis, nucleation and

particle growth, and hydrolysis is the controlling process. Since the photosensitizer $Ru(bpy)_3Cl_2$ were mixed in the hydrolysis system, therefore, $Fe_3O_4@SiO_2(F)$ nanoparticles with the magnetic Fe_3O_4 nanoparticles core and incorporated photosensitizer were formed. The coating of a mesoporous silica layer was realized by base-catalyzed hydrolysis of TEOS in the presence of CTAB [24]. Fig. 1(a) shows the TEM of $Fe_3O_4@SiO_2(F)@meso–SiO_2$ nanoparticles. It can be seen that these nanoparticles have the core-shell structure with the mean diameter of 240 nm. The magnetic Fe_3O_4 nanoparticles core is beneficial to their isolation from the reaction system. After COD was immobilized on $Fe_3O_4@SiO_2(F)@meso–SiO_2$ nanoparticles to form $Fe_3O_4@SiO_2(F)@meso–SiO_2@COD$ nanoparticles, the nanoparticles became more clustered due to the immobilization of COD on their surface (Fig. 1(b)). For the $Fe_3O_4@SiO_2(F)@meso–SiO_2$ nanoparticles, the BET surface area and average pore width were measured to be 563.3 m^2/g and 2.94 nm, respectively. However, after the COD immobilization, the BET surface area of the nanoparticles was measured to be 239.7 m^2/g while the average pore width was measured to be 3.06 nm. The COD immobilization significantly reduced the BET surface area of the nanoparticles, but had less influence on their average pore width. The hysteresis curve shown in Fig. 1(c) indicates that $Fe_3O_4@SiO_2(F)@meso–SiO_2@COD$ nanoparticles are almost superparamagnetic, which is advantageous to their separation and reuse. The addition of fluorescent dye in the nanoparticles is important. The fluorescent dye is sensitive to oxygen based on fluorescence quenching. COD immobilized on the core-shell-structured nanoparticles could catalyze the oxidation of cholesterol. Therefore, this work is to make the foundation for the preparation of the sensing material for fiber optic biosensor based on enzymatic catalysis and oxygen consumption. When excited with light of 350 nm, the water solution containing $Fe_3O_4@SiO_2(F)@meso–SiO_2@COD$ nanoparticles exhibited fluorescence with the maximal wavelength of 610 nm, which was the emission of $Ru(bpy)_3Cl_2$. After oxygen was bubbled into the solution, the fluorescence intensity was decreased with the increase of oxygen bubbled time in the range of 0~50 s and there was a linear relationship between the fluorescence intensity and oxygen bubbled time (Fig. 1(d)). When the oxygen bubbled time was longer than 50 s, the fluorescence intensity kept unchanged due to the saturation of oxygen in solution. These results indicate that $Fe_3O_4@SiO_2(F)@meso–SiO_2@COD$ nanoparticles exhibit good oxygen sensing property in water solution.

FT–IR of $Fe_3O_4@SiO_2(F)@meso–SiO_2@COD$ nanoparticles was determined, as shown in Fig. 2. The peak at 3419 cm^{-1} is assigned to –OH vibration. The band at 1081 cm^{-1} corresponds to Si–O–Si antisymmetric stretching vibrations. The peak at 796 cm^{-1} is associated with the bending vibration of Si-O–Si units [26] and the peak at 959 cm^{-1} is

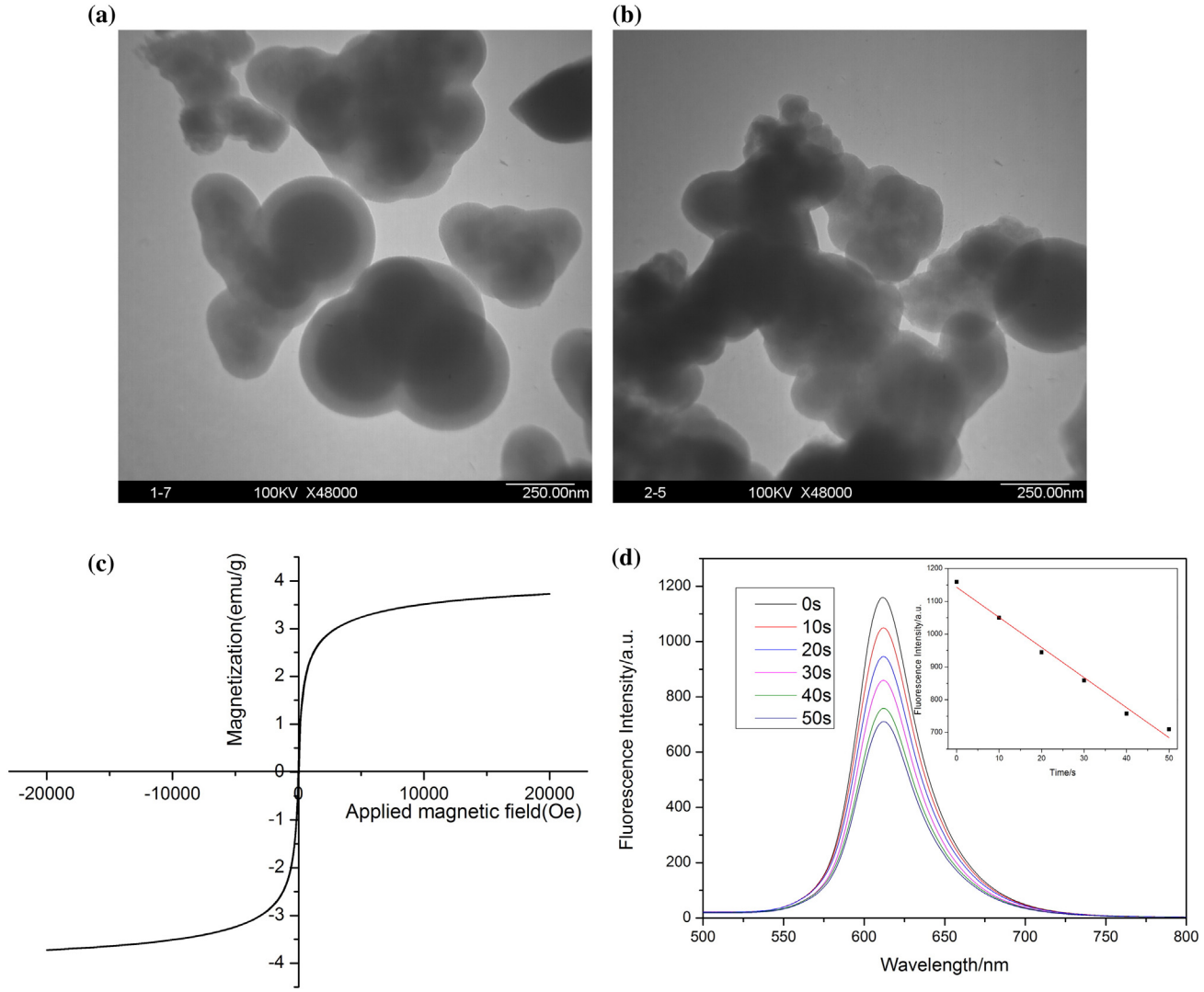

Fig. 1. (a) TEM images of $Fe_3O_4@SiO_2(F)@meso–SiO_2$ nanoparticles (A); (b) TEM image of $Fe_3O_4@SiO_2(F)@meso–SiO_2@COD$ nanoparticles (B); (c) hysteresis curve of B; (d) fluorescence spectra of B after different time of oxygen bubbled into the solution. The inset shows the relationship between fluorescence intensity at 610 nm and oxygen bubbled time.

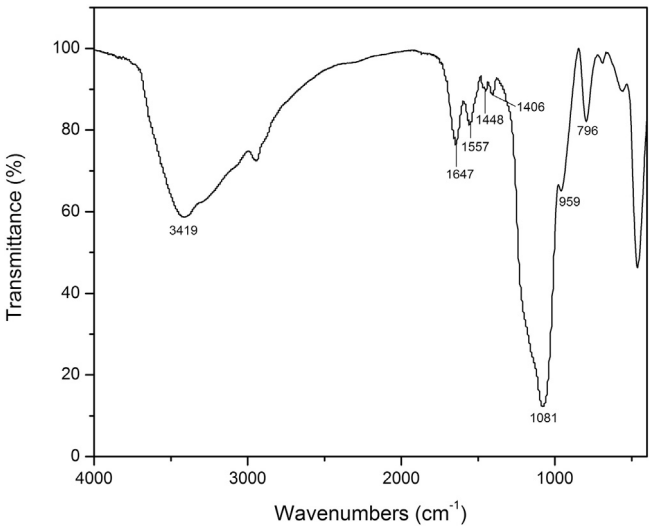

Fig. 2. FT–IR of Fe_3O_4@SiO_2(F)@meso–SiO_2@COD nanoparticles.

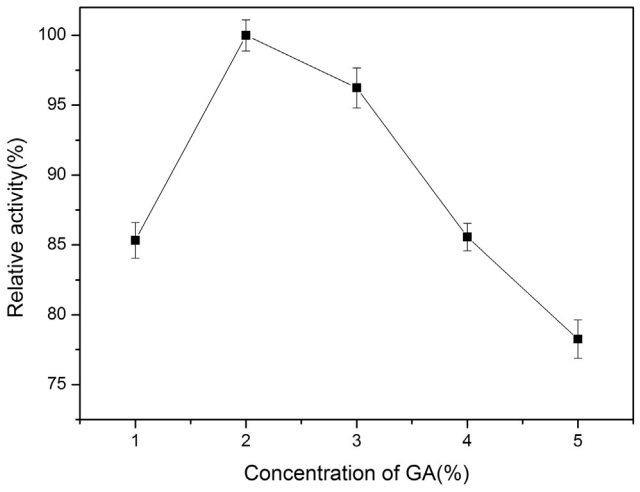

Fig. 4. Effects of GA concentration on activity of Fe_3O_4@SiO_2(F)@meso–SiO_2@COD nanoparticles. APTES concentration: 2.5% (v/v), pH 7.0, COD amount: 10 mg(in 15 mg carrier), T = 25 °C.

assigned to C–N vibration [6]. The characteristic bands of enzyme at 1557 and 1647 cm^{-1} assigned to amide I and amide II, respectively [6,27], were observed in the spectrum. The peak at 1448 cm^{-1} corresponds to the asymmetric bending vibration of enzyme CH_3 group [26]. The peak at 1406 cm^{-1} is associated to typical band of carboxylate groups in the enzyme [27]. Therefore, the immobilization of COD on the nanoparticles was demonstrated.

3.2. Immobilization of COD on Fe_3O_4@SiO_2(F)@meso–SiO_2 nanoparticles

The Immobilization of COD consists of silanization, linker molecule deposition and enzyme coupling, therefore the concentration of APTES and GA, and enzyme amount will have significant effect on COD immobilization. The solution pH also has great influence on the enzyme immobilization due to its effect on the protein charge and crossing-linking process. The effects of APTES concentration on COD immobilization are shown in Fig. 3. It can be seen that with the increase of APTES concentration, the activity of Fe_3O_4@SiO_2(F)@meso–SiO_2@COD nanoparticles increases and reaches its maximal value at APTES concentration of 2.5% (v/v). The activity of the nanoparticles decreases when the APTES concentration is higher than 2.5% (v/v). This is probably due to that higher APTES concentration causes irreversible coagulation and decreases the enzyme activity.

Fig. 4 shows the GA concentration effect on COD immobilization. The optimal GA concentration is 2.0% (v/v) which causes the Fe_3O_4@SiO_2(F)@meso–SiO_2@COD nanoparticles to have the maximal activity. Lower activity of the nanoparticles was observed when GA concentration was lower than 2.0% (v/v). When the GA concentration was too high, a decline in the activity was observed because the cross-linking agent GA is also a protein denaturing agent and will lead to a loss of enzyme activity at higher GA concentration.

The effect of COD amount (in 15 mg carrier) on the Fe_3O_4@SiO_2(F)@meso–SiO_2@COD nanoparticle activity is shown in Fig. 5. The activity was increased with the increase of COD amount and reaches it maximal value at 10 mg. Further increase of COD amount causes the activity of nanoparticle to decrease. The increase of GOD content is in beneficial to enzyme immobilization. However, when GOD content was too high, the enzyme activity would decrease because of the special steric hindrance.

Fig. 6 shows the pH effect on the activity of Fe_3O_4@SiO_2(F)@meso–SiO_2@COD nanoparticles. When the solution pH increases from 5.5 to 7.0, the activity of nanoparticles increases and reaches its maximal value at pH 7.0. Further increase of pH will causes the activity to

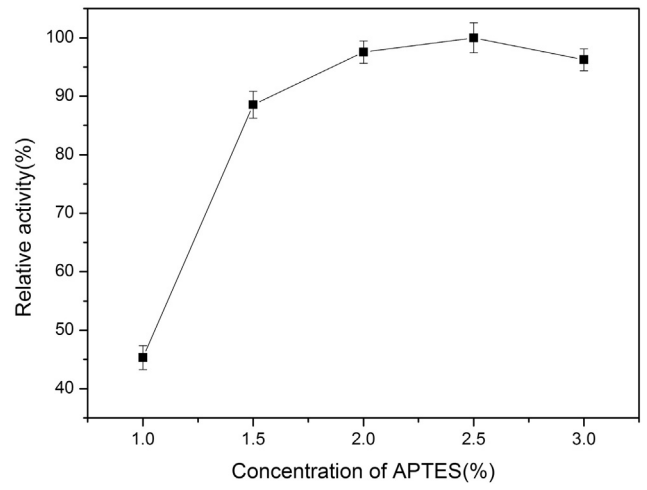

Fig. 3. Effects of APTES concentration on activity of Fe_3O_4@SiO_2(F)@meso–SiO_2@COD nanoparticles. GA concentration: 2.0% (v/v), pH 7.0, COD amount: 10 mg (in 15 mg carrier), T = 25 °C.

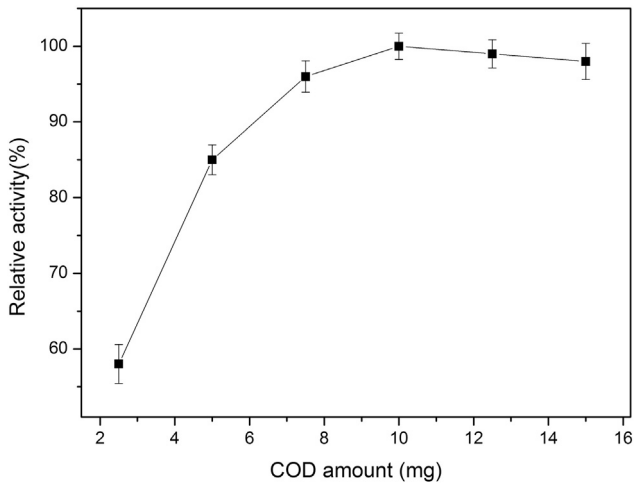

Fig. 5. Effects GOD amount on activity of Fe_3O_4@SiO_2(F)@meso–SiO_2@COD nanoparticles. APTES concentration: 2.5% (v/v), GA concentration: 2.0% (v/v), pH 7.0, T = 25 °C.

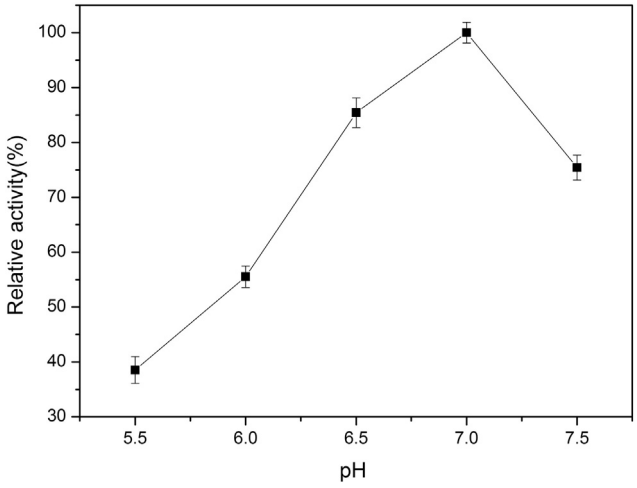

Fig. 6. Effects of pH on activity of Fe_3O_4@SiO_2(F)@meso–SiO_2@COD nanoparticles. APTES concentration: 2.5% (v/v), GA concentration: 2.0% (v/v), COD amount: 10 mg (in 15 mg carrier), T = 25 °C.

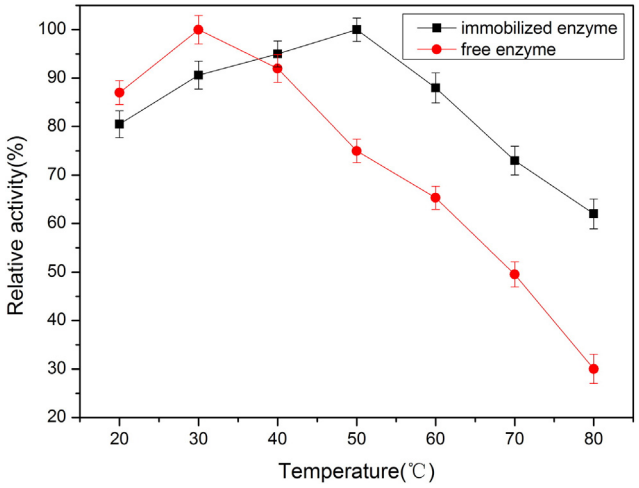

Fig. 8. Effect of temperature on activity of free COD and Fe_3O_4@SiO_2(F)@meso–SiO_2@COD nanoparticles at pH 7.0. The initial activity (the nanoparticles:2000 ± 100 U/g, free COD:20 U/g) is taken as 100%.

decrease. The optimal pH is higher than the isoelectric point (pH 4.9) of free COD and lower than the isoelectric point (pH 8.7) [28] of aminated SiO_2 nanoparticles. In the neutral pH, COD molecules were negatively charged while aminated Fe_3O_4@SiO_2(F)@meso–SiO_2 nanoparticles were positively charged. The free COD absorbed easily on these nanoparticles by electrostatic interaction, which would be beneficial to the increase of immobilized enzyme activity.

After the immobilization, the activity of immobilized COD was detected to be 30 U (2 U in 1 mg carrier), which was about 33.3% of the activity of initial COD. The amount of COD immobilized onto carrier was determined to be 90.8% of the initial COD, giving the immobilized enzyme content of 0.30 mg in 1 mg carrier

3.3. Properties of Fe_3O_4@SiO_2(F)@meso–SiO_2 @COD nanoparticles

It is well known that pH has great effect on enzyme activity. Therefore, the activities of free COD and Fe_3O_4@SiO_2(F)@meso–SiO_2@COD nanoparticles were compared as a function of pH, as shown in Fig. 7. The optimal pH value for free enzyme was found at pH 6.5, and the deviation from optimal pH causes rapid decrease in enzyme activity. The nanoparticles were showed an optimal pH at 7.0. The slight shift of optimal pH value to alkaline region was probably due to the change of its microenvironment caused by the immobilization of COD on carrier. From Fig. 7 it can also be seen that Fe_3O_4@SiO_2(F)@meso–SiO_2@COD nanoparticles has better pH stability than the free one and can be used in a broad pH range. Similar results for immobilization of COD have been reported [29,30].

The temperature effect on the activity of free COD and Fe_3O_4@SiO_2(F)@meso–SiO_2@COD nanoparticles was shown in Fig. 8. The optimal temperature was observed to be 30 °C for free enzyme. On the other hand, the nanoparticles exhibited the optimal activity at 50 °C and a high activity (more than 70% of its initial activity) at the temperature from 20 °C to 70 °C, showing a broad working temperature range. The temperature difference between the free COD and Fe_3O_4@SiO_2(F)@meso–SiO_2@COD nanoparticles is probably due to that the immobilization of enzyme on carrier causes the enzyme to be less susceptible to the temperature-induced conformational change [9].

The thermal stability experiments were performed at 50 °C for free and Fe_3O_4@SiO_2(F)@meso–SiO_2@COD nanoparticles. As shown in Fig. 9, the nanoparticles showed better thermal stability compared to free enzyme. After 5 h incubation, the nanoparticles still retained 80% of its initial activity, while the free enzyme maintained only 47% of its

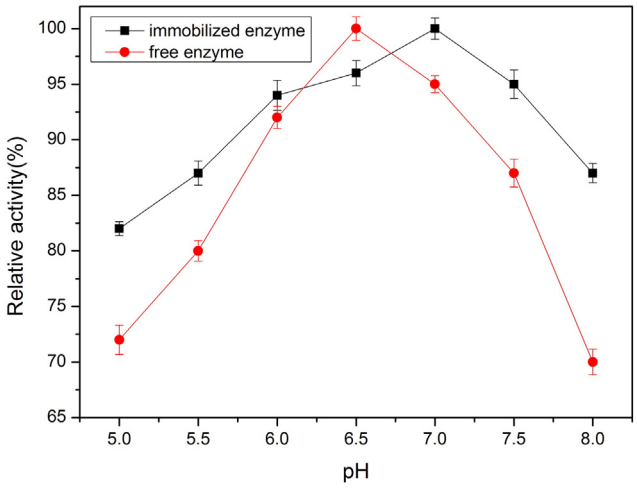

Fig. 7. Effect of pH on activity of free COD and Fe_3O_4@SiO_2(F)@meso–SiO_2@COD nanoparticles at 25 °C. The initial activity (the nanoparticles:2000 ± 100 U/g, free COD:20 U/g) is taken as 100%.

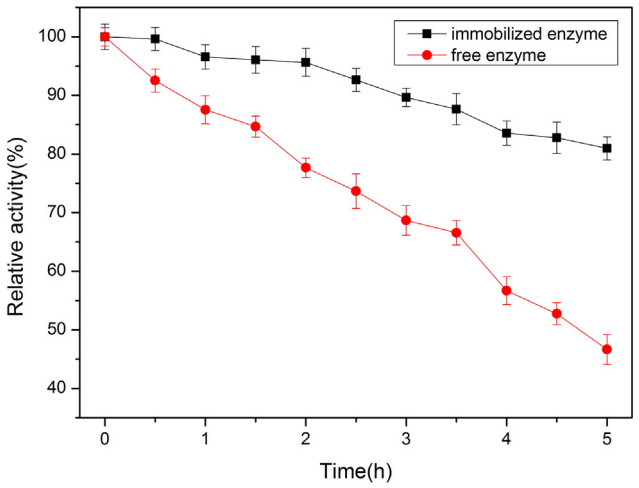

Fig. 9. Thermal stability of free COD and Fe_3O_4@SiO_2(F)@meso–SiO_2@COD nanoparticles at pH 7.0. The initial activity (the nanoparticles: 2000 ± 100 U/g, free COD:20 U/mg) is taken as 100%.

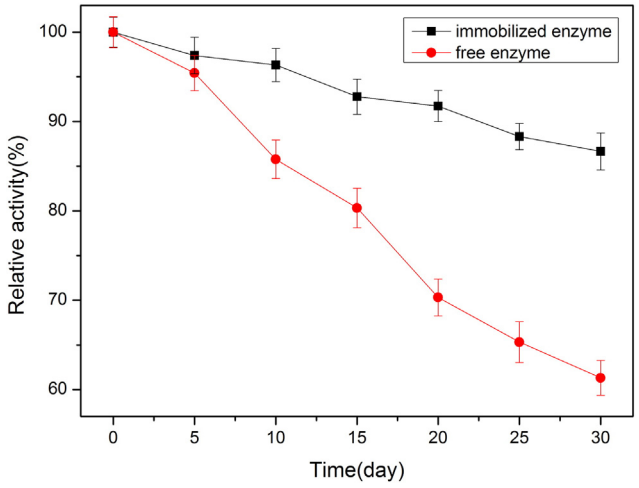

Fig. 10. Storage stability of free COD and Fe_3O_4@SiO_2(F)@meso–SiO_2@COD nanoparticles. The free COD and the nanoparticles were stored in PBS solution (0.2 M, pH 7.0) at 4 °C for 30 days. The activity of enzyme was determined every 5 days. The initial activity (the nanoparticles: 2000 ± 100 U/g, free COD:20 U/mg) is taken as 100%.

initial activity. These can be attributed to the formation of a covalent bond between enzyme and carrier, which prevented the conformation transition of the enzyme [31], therefore leading to an improved thermal stability.

The storage stability experiments were carried out at 4 °C for free and Fe_3O_4@SiO_2(F)@meso–SiO_2@COD nanoparticles and the results are shown in Fig. 10. Under the same conditions, Fe_3O_4@SiO_2(F)@meso–SiO_2@COD nanoparticles decreased at a slower rate compared to the free COD. The nanoparticles maintain 86% of its initial activity after stored for 30 days, while free GOD retains 61% of its initial activity. The storage stability of COD is improved remarkably after the immobilization on the carrier.

The operation stability was investigated due to its importance for repeated application. The main advantage of operation stability is to reduce the cost of the treatment. It can be seen from Fig. 11 that Fe_3O_4@SiO_2(F)@meso–SiO_2@COD nanoparticles maintain 85% of its initial activity after 5 consecutive operations and retain 71% of its initial activity after 7 consecutive operations. The loss of the immobilized enzyme in the repeated operations would probably be one reason for the decrease of its activity.

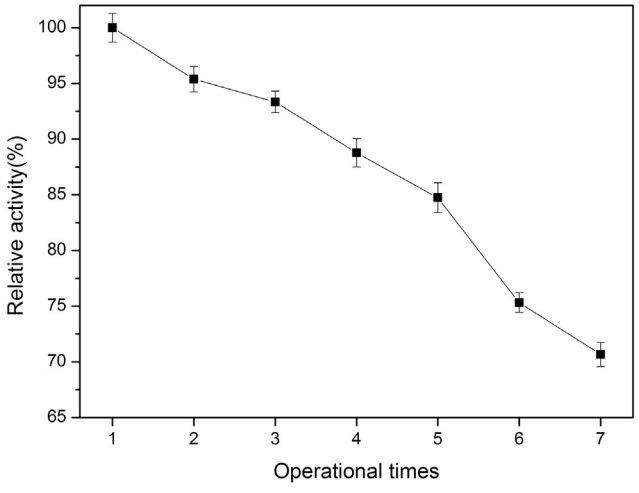

Fig. 11. Operational stability of Fe_3O_4@SiO_2(F)@meso–SiO_2@COD nanoparticles.

4. Conclusion

The magnetic fluorescent core-shell structured nanoparticles were prepared. COD was immobilized on them to form Fe_3O_4@SiO_2(F)@meso–SiO_2@COD nanoparticles and the immobilization conditions were studied. The optimal catalytic pH and temperature for the nanoparticles were 7.0 and 50 °C, respectively. After immobilization, the thermal, storage and operational stabilities of COD were improved. Fe_3O_4@SiO_2(F)@meso–SiO_2@COD nanoparticles might be used as the sensing material in multi parameter fiber optic biosensor based on enzyme catalysis and oxygen consumption.

Acknowledgments

This work was financially supported by National Natural Science Foundation of China (No: 61377092).

References

[1] K.W. Ahn, N.S. Sampson, Cholesterol oxidase senses subtle changes in lipid bilayer structure, Biochemistry 43 (2000) 827–836.
[2] Y. Chen, Y. Xin, H.L. Yang, L. Zhang, Y.R. Zhang, X.L. Xia, Y.J. Tong, W. Wang, Immobilization and stabilization of cholesterol oxidase on modified aepharose particles, Int. J. Biol. Macromol. 56 (2013) 6–13.
[3] E. Yapar, S.K. Kayahan, A. Bozkurt, L. Toppare, Immobilizing cholesterol oxidase in chitosan-alginic acid network, Carbohydr. Polym. 76 (2009) 430–436.
[4] K.K. Gilles, I. Joseph, M. Gregory, Examination of cholesterol oxidase to magnetic nanoparticles, J. Nanobiotechnol. 3 (2005) 1–9.
[5] S.F. Torabi, K. Khajeh, S. Ghasempura, Covalent attachment of cholesterol oxidase and horseradish peroxidase on perlite through silanization: Activity, stability and co-immobilization, J. Nanobiotechnol. 131 (2007) 111–120.
[6] S. Singh, P.R. Solanki, M.K. Pandey, B.D. Malhotra, Covalent immobilization of cholesterol esterase and cholesterol oxidase on polyaniline films for application to cholesterol biosensor, Anal. Chim. Acta 568 (2006) 126–132.
[7] C.C. Lin, M.C. Yang, Cholesterol oxidation using hollow fiber dialyzer immobilized with cholesterol oxidase: preparation and properties, Biotechnol. Prog. 19 (2003) 361–364.
[8] U. Saxena, P. Goswami, Silk Mat as Bio-matrix for the Immobilization of Cholesterol Oxidase, Appl. Biochem. Biotechnol. 162 (2010) 1122–1131.
[9] B. Akkaya, F. Sahin, G. Demirel, H. Tümtürk, Functional polymetric supports for immobilization of cholesterol oxidase, Biochem. Eng. J. 43 (2009) 333–337.
[10] X.J. Wu, M.M.F. Choi, Hydrogel network entrapping cholesterol oxidase and octadecylsilica for optical biosensing in hydrophobic organic or aqueous micelle solvents, Anal. Chem. 75 (2003) 4019–4027.
[11] Suman, C.S. Pundir, Co-immobilization of cholesterol esterase, cholesterol oxidase and peroxidase onto alkylamine glass beads for measurement of total cholesterol in serum, Curr. Appl. Phys. 3 (2003) 129–133.
[12] K. Mural, K. Kato, Development of cholesterol biosensor with high sensitivity using dual-enzyme immobilization into the mesoporous silica materials, Appl. Surf. Sci. 258 (2011) 1725–1732.
[13] A. Kumar, R. Malhotra, B.D. Malhotra, S.K. Grover, Co-immobilization of cholesterol oxidase and horseradish peroxidase in a sol-gel film, Anal. Chim. Acta 414 (2000) 43–50.
[14] Zs. CsoWgor, M. Nacken, M. Sameti, C.-M. Lehr, H. Schmidt, Modified silica particles for gene delivery, Mater. Sci. Eng. C 23 (2003) 93–97.
[15] K.C. de Souza, G.F. Andrade, I. Vasconcelos, I.M. de Oliveira Viana, C. Fernandes, E.M.B. de Sousa, Magnetic solid-phase extraction based on mesoporous silica-coated magnetic nanoparticles for analysis of oral antidiabetic drugs in human plasma, Mater. Sci. Eng. C 40 (2014) 275–280.
[16] R.P. Bagwe, X. Zhao, W. Tan, J. Dispersion, Bioconjugated luminescent nanoparticles for biological applications, Sci. Technol. 24 (2003) 453–464.
[17] W. Schuetz, F. Caruso, Electrostatically assembled fluorescent thin films of rare-earth-doped lanthanum phosphate nanoparticles, Chem. Mater. 14 (2002) 4509–4516.
[18] S. Santra, P. Zhang, K.M. Wang, R. Tapee, W.H. Tan, Conjugation of biomolecules with luminophore-doped silica nanoparticles for photostable biomarkers, Anal. Chem. 73 (2001) 4988–4993.
[19] S. Santra, K.M. Wang, R. Tapee, W.H. Tan, Development of novel dye-doped silica nanoparticles for biomarker application, J. Biomed. Opt. 6 (2001) 160–166.
[20] D.W. Campbell, C. Muller, K.F. Reardon, Development of a fiber optic enzymatic biosensor for 1,2-dichloroethane, Biotechnol. Lett. 28 (2006) 883–887.
[21] H. Endo, Y. Yonemori, K. Musiya, M. Maita, T. Shibuya, H. Ren, T. Hayashi, K. Mitsubayashi, A needle-type optical enzyme sensor system for determining glucose levels in fish blood, Anal. Chim. Acta 573-574 (2006) 117–124.
[22] K.F. Reardon, D.W. Campbell, C. Muller, Optical fiber enzymatic biosensor for reagentless measurement of ethylene dibromide, Eng. Life Sci. 9 (2009) 291–297.
[23] T. Massart, Preparation of aqueous magnetic liquids in alkaline and acidic media, IEEE Trans. Magn. 17 (1981) 1247–1248.
[24] W. Stöber, A. Fink, E. Bohn, Controlled growth of monodisperse silica spheres in the micron size range, J. Colloid Interface Sci. 26 (1968) 62–69.

[25] M.M. Bradford, A rapid and sensitive method for the quantitation of microgram quantities of protein utilizing the principle of protein-dye binding, Anal. Biochem. 72 (1976) 248–254.
[26] S. Singh, R. Singhal, B.D. Malhotra, Immobilization of cholesterol esterase and cholesterol oxidae onto sol-gel films for application to cholesterol biosensor, Anal. Chim. Acta 582 (2007) 335–343.
[27] F. Šulek, Ž. Knez, M. Habulin, Immobilization of cholesterol oxidase to finely dispersed silica-coated maghemite nanoparticles based magnetic fluid, Appl. Surf. Sci. 256 (2010) 4596–4600.
[28] Z. Wu, H. Xiang, T. Kim, M.S. Chun, K. Lee, Surface properties of submicrometer silica spheres modified with aminopropyltriethoxysilane and phenyltriethoxysilane, J. Colloid Interface Sci. 304 (2006) 119–124.
[29] S. Singh, A. Chaubey, B.D. Malhorra, Amperometric cholesterol biosensor based on immobilized cholesterol esterase and cholesterol oxidase on conducting polypyrrole films, Anal. Chim. Acta 502 (2004) 229–234.
[30] C.C. Lin, M.C. Yang, Cholesterol oxidation using hollow fiber dialyzer immobilized with cholesterol: effect of storage and reuse, Biomaterials 24 (2003) 549–557.
[31] F. Sahin, G. Demirel, H. Tumturk, A novel matrix for the immobilization of acetylcholinesterase, Int. J. Biol. Macromol. 37 (2005) 148–153.